Transverse and longitudinal polarized-neutron, polarized-^{93}Nb scattering, and the tensor spin-spin potential

J. P. Soderstrum,[1,*] C. R. Gould,[1] D. G. Haase,[1] N. R. Roberson,[2] M. B. Schneider,[3,†] and L. W. Seagondollar[1]

[1] *North Carolina State University, Raleigh, North Carolina 27695 and Triangle Universities Nuclear Laboratory, Durham, North Carolina 27706*

[2] *Duke University, Durham, North Carolina 27706 and Triangle Universities Nuclear Laboratory, Durham, North Carolina 27706*

[3] *University of North Carolina, Chapel Hill, North Carolina 27514 and Triangle Universities Nuclear Laboratory, Durham, North Carolina 27706*

(Received 16 May 1991)

Spin-spin cross sections were measured for 7.5-MeV polarized neutrons incident on cryogenically polarized ^{93}Nb. Measurements were made with spin orientations transverse and longitudinal to the beam direction, yielding $\sigma_T^{ss} = -5.2 \pm 5.3$ mb and $\sigma_L^{ss} = -2.2 \pm 6.9$ mb, respectively. The results are consistent with recent valence-nucleon folding model calculations. The tensor spin-spin potential is found to be small, $V_{12} = -67 \pm 190$ keV. Volume integrals of spin-spin potentials are derived from depolarization and transmission experiments on ^{13}C, ^{15}N, ^{27}Al, and ^{93}Nb. The results for the central spin-spin potential are shown to be consistent with the folding model predictions.

PACS number(s): 25.40.Dn, 24.10.Ht, 24.70+s

I. INTRODUCTION

Studies of spin-spin effects in polarized nucleon scattering now show unambiguous evidence for the existence of a nucleon-nucleus spin-spin interaction. The experiments are of two types: transmission of polarized neutrons through polarized targets, and proton depolarization in elastic scattering from spin-$\frac{1}{2}$ targets. Gould *et al.* [1] studied polarized neutron transmission through polarized ^{27}Al with neutrons of energy 5–16 MeV, and Heeringa *et al.* [2] studied polarized-neutron transmission through polarized ^{27}Al and ^{93}Nb with neutrons of energy 20–50 MeV. Przewoski *et al.* [3] studied proton depolarization for ^{13}C at 72 MeV, and Nakano *et al.* [4] studied proton depolarization for ^{15}N at 65 MeV.

The measurements are analyzed in terms of central and tensor spin-spin potentials [5]. Following the notation of McAbee *et al.* [6], these are given by

$$U_{10}(\mathbf{r}) = -F_{10}(\mathbf{r})\hat{\mathbf{I}} \cdot \hat{\mathbf{s}} \tag{1}$$

and

$$U_{12}(\mathbf{r}) = -F_{12}(\mathbf{r})[3(\hat{\mathbf{I}} \cdot \hat{\mathbf{r}})(\hat{\mathbf{s}} \cdot \hat{\mathbf{r}}) - (\hat{\mathbf{I}} \cdot \hat{\mathbf{s}})]/2 \ , \tag{2}$$

where $\mathbf{I}$ is the target spin, $\mathbf{s}$ is the nucleon spin, $\mathbf{r}$ is the nucleon-nucleus separation vector, and F_{10} and F_{12} are geometric factors describing the shapes of the central and tensor potentials. The potentials are unit normalized ($\hat{\mathbf{I}} = \mathbf{I}/I$, etc.). For targets with $I > \frac{1}{2}$ additional spin-spin terms arise [6] due to higher-order polarization moments in the target. In general though, the dominant terms are U_{10} and U_{12}, involving the target spin I to first order.

The geometric factors $F_{ik}(\mathbf{r})$ may have a complicated radial dependence. Commonly the potentials are taken to have volume or derivative Woods-Saxon shapes. In this case $F_{ik}(\mathbf{r}) = V_{ik}f(r)$, and V_{10} and V_{12} parametrize the strengths of the central and tensor potentials, respectively.

From analysis of ^{15}N depolarization data, Nakano *et al.* [4] found the tensor potential to be large. They concluded that V_{12} was of order 0.8 MeV or more. The ^{93}Nb data of Heeringa *et al.* [2] could also be interpreted in terms of a large tensor potential $V_{12} \sim 2$ MeV. However, the measurements do not readily distinguish the effects of the central and tensor terms. Solutions with predominantly central potentials also gave reasonable accounts of the data.

A technique for resolving this ambiguity, first discussed by Fisher [7], involves polarized-neutron, polarized-target transmission in two geometries: transverse (with the spins perpendicular to the beam direction) and longitudinal (with the spins parallel to the beam direction). The spin-spin cross section is obtained from the change in the transmission when the neutron spin is flipped with respect to the target spin. The central contribution is the same in the two geometries. The tensor contribution changes in sign and magnitude between transverse and longitudinal. As a result the tensor contribution can be extracted unambiguously from the cross-section difference between the two geometries.

Previous measurements were carried out only in trans-

*Present address: EG&G Energy Measurements, PO Box 1912, Las Vegas, NV 89125.

†Present address: Physics Dept., Grinnell College, Grinnell, IA 50112.

verse geometry. In the present work we report the first measurement with spins in both transverse and longitudinal geometry. The target was ^{93}Nb, and the measurements were carried out at 7.5-MeV neutron energy, where optical model calculations [2] and folding model calculations [6] indicate the effect of the tensor term is a local maximum. Although the measured cross sections proved to be small, they set a bound on the tensor potential which rules out the large tensor potential solution obtained in the work of Heeringa *et al.* [2].

Mcabee *et al.* [6] have recently used modern effective interactions to carry out a theoretical study of spin-spin effects using the valence-nucleon folding model. Our results are in qualitative agreement with these new calculations. We also compare the volume integrals of the central and tensor spin-spin potentials found in the recent depolarization and transmission measurements. Despite the large differences in mass number, the results are consistent, and in surprisingly good agreement with the new calculations.

II. EXPERIMENTAL PROCEDURE

The experimental procedures are similar to those described in our earlier work [1, 8]. A schematic of the experimental arrangement is shown in Fig. 1. Deuterons from the Triangle Universities Nuclear Laboratory Lamb shift polarized ion source [9] and FN tandem Van de Graaff accelerator were focused into a 6-cm-long gas cell filled with 8 atm of deuterium. A double steerer-feedback system centered the beam in front of the gas cell, and on a beam profile monitor 2 m upstream. Polarized neutrons were produced from the ^{2}H($\vec{d}$,$\vec{n}$) reaction and were collimated at zero degrees by a 0.95-cm-diameter aperture in a polyethylene shield. The neutrons passed through the polarized niobium sample and were detected 2.3 m away in a heavily shielded 13-cm-diameter by 13-cm-long NE213 liquid scintillator. The neutron flux from the gas cell was monitored by a 1.3-cm-diameter by 1.9-cm-long NE213 scintillator, placed inside the polyethylene collimator, 53 cm from the gas cell. Deuteron polarizations were typically 60–70 %, resulting in neutron polarizations of 50–60%. The energy spread in the neutron beam was about 700 keV, due to energy loss of the deuterons in the gas cell.

The niobium target was pure metal, 1.8 cm thick by 1.8 cm wide by 3.8 cm high. The target was cryogenically polarized by a 10-mK dilution refrigerator system and a 7-T split-pole superconducting magnet. The apparatus is described in more detail by Haase *et al.* [10]. The magnet has a main bore 10.2 cm in diameter, and four 90° access ports, 4.13 cm in diameter. The ports allow the magnet to be oriented in the horizontal plane with the field axis either parallel or perpendicular to the beam direction. The target temperature was typically 10 mK and was monitored by the decay from a ^{60}Co(Co) single crystal source mounted to the base of the sample. For ^{93}Nb at 10 mK, the three lowest-order nuclear orientation parameters [11] $B_i(I)$ are $B_1 = -0.84$, $B_2 = 0.35$, and $B_3 = -0.093$. The vector polarization of the target is given by $P_t = -\sqrt{(I+1)/3I}B_1$. This is the only orientation parameter of interest in the present experiment; our measurement is not sensitive to even rank nuclear orientations, and third-order orientation is negligible to within the accuracy of the experiment ($B_3/B_1 = 0.11$).

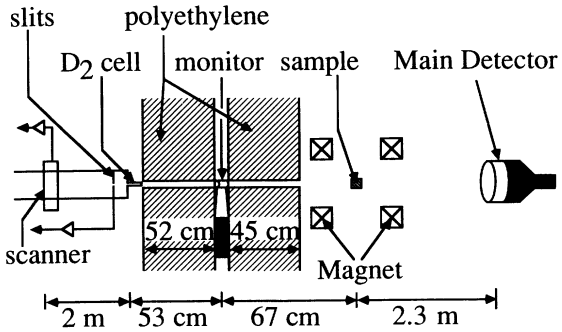

FIG. 1. Schematic diagram of the experimental arrangement.

With 100 nA of deuterons on the gas cell, count rates for neutrons were 2.2 kHz in the monitor detector and 1.0 kHz in the main detector. Neutron and γ-ray events in the scintillators were separated by pulse shape discrimination. Dead-time corrections and gain stabilization were made using pulsed LED light fed directly to the photocathodes of the photomultiplier tubes for each detector. In order to avoid counting low-energy neutrons from deuteron break-up reactions, a single channel analyzer (SCA) window was set on the upper region of each proton recoil spectrum. The SCA outputs were stored in scalers along with LED pulser information to calculate the dead times, typically 1.5 μs per event.

For each measurement between 50 and 100 runs were taken with the target cold, followed by an equal number of runs with the target depolarized by warming to 0.5 K. Each run consisted of eight 200-s spin sequences, with the target and projectile spins alternately aligned parallel and antiparallel. The neutron spin was reversed by flipping the spin of the deuteron in the polarized source. This reverses the vector polarization, P_z, of the deuteron beam, and in principle leaves the tensor polarization, P_{zz}, unchanged.

The asymmetry is defined as

$$\epsilon = (N_p - N_a)/(N_p + N_a) \tag{3}$$

with N_p (N_a) the monitor normalized counts in the parallel (antiparallel) spin configuration. We derive a spin-spin cross section from the cold and warm asymmetries using

$$\sigma^{ss} = -(\epsilon_{\rm cold} - \epsilon_{\rm warm})/P_b P_t x \ , \tag{4}$$

where $P_b = 0.57$ (0.55) is the average longitudinal (transverse) neutron beam polarization, calculated from the measured deuteron polarization and the polarization transfer coefficients for the ^{2}H($\vec{d}$,$\vec{n}$) reaction; $P_t = 0.50$ is the average target polarization, calculated from the target temperature; and x is the sample thickness, 0.10 atom/b.

Table I gives the cold and warm asymmetries measured

TABLE I. Cold and warm asymmetries measured for 7.5-MeV polarized neutron scattering from polarized ^{93}Nb in transverse and longitudinal geometries. The errors are derived from the spread in the individual asymmetries from each run. The experimentally derived spin-spin cross sections, $\sigma_{\rm ex}^{ss}$, are shown in column 4. The valence-nucleon folding model predictions of Ref. [6], $\sigma_{\rm th}^{ss}$, are shown in column 5.

Geometry	$<\epsilon>_{\rm cold}$ (10^{-4})	$<\epsilon>_{\rm warm}$ (10^{-4})	$\sigma_{\rm ex}^{ss}$(mb)	$\sigma_{\rm th}^{ss}$(mb)
Transverse	3.39 ± 0.91	1.99 ± 0.92	-5.2 ± 5.3	-13.5
Longitudinal	-8.81 ± 1.28	-9.43 ± 1.46	-2.2 ± 6.9	-5.5

in the two geometries. The errors are derived from the standard deviation of the individual asymmetries in each data set. These errors were comparable to the errors expected on the basis of counting statistics (average $\chi^2 \sim 0.96$), indicating no large nonstatistical fluctuations. The typical uncertainty of 10% in the polarizations is small compared to the relative statistical uncertainties in the asymmetries.

The warm asymmetries are close to zero for the transverse data but not for the longitudinal data. We believe this is due to few percent differences in the the tensor polarization P_{zz} of the deuteron beam when the deuteron spin is flipped. A similar problem was noted in Ref. [2]. The neutron yield depends on P_{zz} and is more sensitive to P_{zz} in longitudinal geometry than in transverse geometry [12]. If P_{zz} changes coherently between the two spin states, a nonzero neutron asymmetry results, unrelated to spin-spin effects. The monitor should correct for this changing yield, but does not, due to slight differences in the beam profile subtended at the monitor and main detector locations. Warming the target leaves this effect unchanged, and subtracting the warm asymmetry from the cold asymmetry reliably corrects for this systematic difference [13].

III. ANALYSIS OF ^{93}Nb RESULTS

The spin-spin cross sections derived from the longitudinal and transverse asymmetries are shown in column 4 of Table I. The values are small, establishing the cross sections to be less than 10 mb in both geometries.

The cross sections can be compared directly to the recent distorted-wave Born approximation calculations of McAbee *et al.* [6]. These authors used a valence-nucleon model and modern effective nucleon-nucleon interactions with exchange to derive spin-spin cross sections. The nucleus ^{93}Nb has one proton above the $Z = 40$ shell closure and the valence-nucleon model is expected to give a reliable description of the spin-spin interaction. The predictions are shown in column 5 of Table I. The measured transverse cross section is smaller than the predicted value, but overall the experimental bounds are consistent with the model predictions. Similar agreement in transverse geometry was noted by Heeringa *et al.* [2].

More insight into the relative contributions of the central and tensor potentials can be gained by writing the spin-spin cross sections σ^{ss} in terms of the spin-spin analyzing cross sections σ_{10}^{ss} and σ_{12}^{ss} defined by McAbee *et al.* [6]. In the limit of no spin-orbit coupling, the cross section σ_{10}^{ss} is due to the central spin-spin potential V_{10}, and the cross section σ_{12}^{ss} is due to the tensor spin-spin potential V_{12}. We neglect the σ_{32}^{ss} contribution because, as mentioned earlier, the rank-three orientation parameter $B_3(I)$ is small. For the target and beam polarization axes parallel and at angle θ with respect to the beam direction, the general form of equation 2.25 of McAbee *et al.* [6] is then

$$\sigma^{ss}(\theta) = B_1(I)B_1(\tfrac{1}{2}) \sum_k \sigma_{1k}^{ss} P_k(\cos\theta). \tag{5}$$

The longitudinal ($\theta = 0$) and transverse ($\theta = \pi/2$) spin-spin cross sections can then be written as

$$\begin{aligned} \sigma_L^{ss} &= (\sigma_{10}^{ss} + \sigma_{12}^{ss})K \ , \\ \sigma_T^{ss} &= (\sigma_{10}^{ss} - \sigma_{12}^{ss}/2)K \ , \end{aligned} \tag{6}$$

where $K = \sqrt{3I/(I+1)}P_b P_t$ for a target with spin I. We set $P_b = P_t = 1$ to compare with the spin-spin cross sections of Table I. For ^{93}Nb with $I = \frac{9}{2}$ we have $K = 1.57$, giving

$$\sigma_{10}^{ss} = \tfrac{1}{3}(\sigma_L^{ss} + 2\sigma_T^{ss})/1.57 = -2.7 \pm 2.7 \text{ mb} \tag{7}$$

and

$$\sigma_{12}^{ss} = \tfrac{2}{3}(\sigma_L^{ss} - \sigma_T^{ss})/1.57 = 1.3 \pm 3.7 \text{ mb}. \tag{8}$$

The valence model predictions are $\sigma_{10}^{ss} = -7.6$ mb and $\sigma_{12}^{ss} = 3.3$ mb. The experimental 1σ limit for the central term is somewhat smaller than the predicted value, but the tensor bound is quite consistent with the model.

To relate these spin-spin analyzing cross sections to potentials we now consider spherical optical model descriptions of the data. Heeringa *et al.* [2] found two equally satisfactory optical model solutions to the spin-spin cross section data for ^{93}Nb: one solution with only a central spin-spin term, the other with only a tensor spin-spin term. Our measurements allow us to rule out the tensor potential solution.

From their Fig. 2 we see that at 7.5 MeV, with V_{10} zero and $V_{12} = -2160$ keV, σ_T^{ss} is calculated to be -33 mb. From Eq. (6), therefore, σ_{12}^{ss} is predicted to be 42 mb. This is much larger than our measured value of 1.3 ± 3.7 mb, and a large tensor potential is therefore not consistent with our data. In terms of the geometry used by Heeringa *et al.* [2] our measurements imply $V_{12} = -67 \pm 190$ keV.

A similar scaling of their central potential solution yields $V_{10} = 460 \pm 460$ keV from our σ_{10}^{ss} measurement, in agreement with their central spin-spin solution

of $V_{10} = 1090 \pm 230$ keV. The ^{93}Nb spin-spin data taken together are therefore well described by a predominantly central spin-spin potential of order 1 MeV, with a small tensor spin-spin potential of at most a few hundred keV.

IV. COMPARISON OF POTENTIALS FOR ^{13}C, ^{15}N, ^{27}Al, AND ^{93}Nb

Here we compare the spin-spin potentials for ^{93}Nb relative to potentials found for ^{13}C, ^{15}N, and ^{27}Al. Because of the differences in geometries, we consider volume integrals of the potentials rather than potential depths directly. This is a more appropriate measure because, as argued by McAbee *et al.* [6], cross sections for low-momentum processes are more sensitive to volume integrals than to well depths.

The signs of the volume integrals are of interest. These are determined in transmission experiments because the asymmetry depends on the spin-spin potentials in first order. Overall signs are not determined in depolarization experiments because the observable is sensitive to the spin-spin interaction only in second order. However, the relative sign between the central and tensor terms can in principle be determined.

First, we consider the central spin-spin potentials. In the valence model, the volume integral, J_{10}, of the central spin-spin potential, V_{10}, is related to the volume integral, $J_{\sigma\sigma}$, of the central spin-spin term, $v_{\sigma\sigma}$ of the effective nucleon-nucleon interaction [14]. Explicitly,

$$J_{10} \equiv 4\pi V_{10} \int f(r) r^2 dr = -I/(\ell + 1/2) J_{\sigma\sigma}. \qquad (9)$$

Here we have adapted the expression given by Nakano *et al.* [4] to include a factor of I for unit-normalized potentials. We also include a phase factor $(-1)^{I-(\ell+1/2)}$ (I half integer) to take into account the change in sign of the potential depending on whether the valence nucleon has $j \equiv I = \ell \pm \frac{1}{2}$. We take $J_{\sigma\sigma}(nn,pp) = 283$ MeV fm^3, and $J_{\sigma\sigma}(np) = -213$ MeV fm^3 from the recent work of McAbee *et al.* [6]. The comparison of the theoretical and experimental volume integrals J_{10} is given in Table II. The signs are in agreement. The experimental values tend to be slightly larger than the theoretical values and, for ^{13}C, the value is about a factor of 2 too large. However, Przewoski *et al.* [3] pointed out that even a small tensor potential $V_{12} = 25$ keV changed their central potential V_{10} solution significantly, from 350 to 250 keV. We conclude therefore that a smaller value of J_{10} is easily accommodated for ^{13}C, and similarly for the other nuclei.

Interestingly, the overall agreement would have been poor using the early phenomenological value [5] of $J_{\sigma\sigma}(np) = -45$ MeV fm^3. If the ambiguities between central and tensor potentials can be resolved, it is clear that proton depolarization measurements and polarized neutron transmission measurements can show good sensitivity to the values of the volume integrals of the effective interactions.

Second, we consider the volume integrals J_{12} of the tensor potentials V_{12}. No simple scaling law equivalent to Eq. (9) has been given, but McAbee *et al.* [6] have suggested that in the limit of no spin-orbit distortion, $\sigma_{12}^{ss}/\sigma_{10}^{ss} \approx -1/(2 + 3/\ell)$ for a target with $I = \ell + \frac{1}{2}$, and $\sigma_{12}^{ss}/\sigma_{10}^{ss} \approx 1/2(1 + \frac{1}{2}\ell)$ for a target with $I = \ell - \frac{1}{2}$. This implies values of $J_{12}/J_{10} \approx -\frac{1}{3}$ for ^{27}Al and ^{93}Nb, and $J_{12}/J_{10} \approx +\frac{3}{4}$ for ^{15}N. Our value of $V_{12} = -67 \pm 190$ keV for ^{93}Nb gives $J_{12} = 74 \pm 211$ MeV fm^3, consistent in magnitude with the scaling law ($J_{10} \sim 300$ MeV fm^3 from Table II). Of course we cannot confirm the sign change. The large tensor potentials found by Nakano *et al.* [4] in ^{15}N correspond to volume integrals $J_{12} = -255$ and 365 MeV fm^3 respectively (sets III and IV respectively). The scaling law prefers the set III potential solution (same sign for J_{10} and J_{12}), but the magnitude of J_{12} appears about a factor of 2 too large compared with the J_{10} value of -133 MeV fm^3.

Roy *et al.* [16] found a nonzero tensor potential from proton depolarization measurements on ^{9}Be. In their calculations, the central and tensor potentials were of comparable strength, $V_{12} \approx V_{10} \approx 1.2$ MeV. The analysis is more complicated than for ^{13}C and ^{15}N, however. The target spin is $\frac{3}{2}$, and quadrupole spin-flip contributes significantly to the depolarization.

We conclude that while current experiments do show indications of a tensor spin-spin potential, more quantitative comparisons with theory will require additional

TABLE II. Volume integrals, J_{10} in units of MeV fm^3 for central spin-spin potentials in ^{13}C, ^{15}N, ^{27}Al, and ^{93}Nb. The theoretical values J_{10}^{theory} in column 6 are calculated from Eq. (9), using $J_{\sigma\sigma}$ values from Ref. [6]. The experimental values J_{10}^{expt} in column 7 are calculated from unit-normalized potentials, V_{10} derived from potentials given in Refs. [2–4].

Nucleus	I	ℓ	$J_{\sigma\sigma}$	J_{10}^{theory}	J_{10}^{expt}
^{13}C	$\frac{1}{2}$	1	−213	71	140 ± 20[a]
^{15}N	$\frac{1}{2}$	1	283	−94	-133 ± 7[b]
^{27}Al	$\frac{5}{2}$	2	−213	213	237 ± 98[c]
^{93}Nb	$\frac{9}{2}$	4	−213	213	337 ± 71[c]

[a] Reference [3].
[b] Set III from Ref. [4].
[c] Reference [2].

measurements that can unambiguously separate the effects of the central and tensor terms.

V. CONCLUSIONS

We have reported the first measurements of spin-spin analyzing cross sections in transverse and longitudinal geometries. The measurements allow a separation of central and tensor spin-spin contributions to the neutron-nucleus potential. The tensor spin-spin potential in ^{93}Nb is found to be small: $V_{12} = -67 \pm 190$ keV. However, the results are consistent with recent valence-nucleon folding model calculations which use a large value of the n-p spin-spin effective interaction.

We have considered all recent data on spin-spin effects and find agreement in sign and magnitude with the predictions of the valence model for the central spin-spin term. The positive tensor spin-spin term found for ^{15}N by Nakano *et al.* [4] is consistent in sign with the predictions of the valence model, but larger than expected. More quantitative comparisons of the tensor spin-spin term await additional precise measurements in other nuclei.

It is clear that if the ambiguities between central and tensor contributions can be resolved, accurate depolarization and transmission measurements, such as those recently reported, can show good sensitivity to the strength of the underlying spin-spin effective N-N interaction.

ACKNOWLEDGMENTS

We thank W. J. Thompson and T. L. McAbee for valuable discussions and for providing the results of the valence model calculations at 7.5 MeV. We thank K. Nash and J. Koster for their assistance in taking the data, and P. Huffman for performing calculations. This work was supported in part by the U. S. Department of Energy, Office of High Energy and Nuclear Physics, under Contract Nos. DE-AC05-76ER01067 and DE-FG05-88ER40441, and by the U. S. Department of Energy, Office of Energy Research, under Contract No. W-7405-ENG-36.

[1] C. R. Gould, D. G. Haase, L. W. Seagondollar, J. P. Soderstrum, K. E. Nash, M. B. Schneider, and N. R. Roberson, Phys. Rev. Lett. **57**, 2371 (1986).

[2] W. Heeringa, H. O. Klages, Chr. Wölfli, and R. W. Finlay, Phys. Rev. Lett. **63**, 2456 (1989).

[3] B. v. Przewoski, P. D. Eversheim, F. Hinterberger, U. Lahr, J. Campbell, J. Götz, M. Hammans, G. Masson, I. Sick, and W. Bauhoff, Phys. Rev. Lett. **64**, 368 (1990).

[4] T. Nakano, M. Nakamura, H. Sakaguchi, M. Yosoi, M. Ieri, H. Togowa, S. Hirata, O. Kamigaito, H. M. Shimizu, M. Iwaki, Y. Nakai, S. Kobayashi, T. Noro, and H. Ikegami, Phys. Lett. B **240**, 301 (1990).

[5] A. H. Hussein and H. S. Sherif, Phys. Rev. C **8**, 518 (1973).

[6] T. L. McAbee, W. J. Thompson, and H. Ohnishi, Nucl. Phys. **A509**, 39 (1990).

[7] T. R. Fisher, Phys. Lett. **35B**, 573 (1971).

[8] J. P. Soderstrum, C. R. Gould, D. G. Haase, L. W. Seagondollar, M. B. Schneider, and N. R. Roberson, Phys. Rev. C **38**, 2424 (1988).

[9] T. B. Clegg, G. A., Bissinger, and T. A. Trainor, Nucl. Instrum. Methods **A120**, 445 (1974).

[10] D. G. Haase, C. R. Gould, and L. W. Seagondollar, Nucl. Instrum. Methods **A243**, 305 (1986).

[11] K. S. Krane, Nucl. Data Tables **11**, 407 (1973).

[12] J. E. Simmons, W. E. Broste, G. P. Lawrence, J. L. McKibben, and G. G. Ohlsen, Phys. Rev. Lett. **27**, 113 (1971).

[13] The close agreement of the errors derived from the standard deviations and the errors derived from counting statistics shows that the tensor polarization is not drifting uncontrollably during a sequence of runs, or during the change from cold to warm data acquisition.

[14] G. R. Satchler, Part. Nuclei **1**, 397 (1971).

[15] Note that the sign of F_{12}/F_{10} in equation 3.2 of Ref. [6] should be positive, not negative.

[16] G. Roy, H. S. Sherif, E. D. Cooper, L. G. Greeniaus, G. A. Moss, J. Soukup, G. M. Stinson, R. Abegg, D. P. Gurd, D. A. Hutcheon, R. Liljestrand, and C. A. Miller, Nucl. Phys. **A442**, 686 (1985).